STRANGE FORM FACTORS OF THE PROTON : RESULTS FROM HAPPEX AT JEFFERSON LAB

E. BURTIN

Service de physique nucléaire
CEA-DSM/DAPNIA
F-91191 Gif sur Yvette, FRANCE.
E-mail: eburtin@cea.fr

representing the Jefferson Lab Hall A Collaboration

The HAPPEX experiment at Jefferson Lab has measured the parity violating asymmetry, $\mathcal{A}_{\rm PV}$, in the scattering of longitudinally polarized electrons off a proton target. This experiment used the two high-resolution spectrometers in the Hall A. Experimental techniques to measure asymmetries of 5 ppm were developed. Data taken at a beam energy of 3.355 GeV and an average Q^2 of 0.48 (GeV/c)^2 shows that the contribution of strange quarks to the proton form factors $G_E^s + 0.39 G_M^s = 0.016 \pm 0.049$ where the error is dominated by statistics. The dominant systematic errors are from the beam polarization and from the knowledge of the neutron electric form factor.

1 A strange proton

1.1 Concepts

The inner structure of a proton can be seen by two complementary manners depending at which scale it is probed. Experiments at high momentum transfers (very fine probe) are precisely described in the framework of quantum chromodynamics, QCD, the fundamental interaction which couples quarks and gluons. On the other side, static properties of most of the hadrons are describable using a classification similar to Mendeleiev's classification of atoms but based on elementary bricks known as constituent quarks.

To reconcile both approaches Kaplan and Manohar proposed [1] that *"a constituent quark comprises a QCD quark surrounded by a complicated mess of glue and $q\bar{q}$ pairs"*. To test this proposition they suggested to measure as many proton matrix elements as possible as possible as well as measuring strange contribution to these matrix elements. In fact, as a proton is made of two constituent up quarks and one down quark, any contribution from strangeness would favor that proposition. Moreover, contributions from heavier quarks are found to be highly suppressed.

1.2 Experimental overview

Since the EMC puzzling result on the spin structure of the nucleon was published [2] there has been a growing interest for seeking strange quarks observable in ordinary matter. Experimental clues have been gathered in various fields but none of them has given a strong evidence of the importance of strange quarks. Among these, experiments conducted with neutrino and anti-neutrino beams [3,4] have lead to the conclusion that 3 % of the momentum of a nucleon is carried by strange quarks. They had also shown that the x_{Bj} distribution of strange and anti-strange quarks were identical within errors.

Other experiments, namely π-N scattering, which had been completed in the past were reanalyzed [5] and their results tend to prove that strangeness might account from 0 to 15 % of the mass of a nucleon depending on which type of analysis is performed.

Recently, experiments studying polarized deep inelastic scattering of leptons off polarized nucleons were conducted at CERN [6], SLAC [7] and DESY [8]. Their results, using SU(3) symmetry, suggest that the strange axial matrix element $< N|\bar{s}\gamma_\mu\gamma_5 s|N >$ is non-zero. Though, there is a strong belief that gluons might contribute to this matrix element and then infirm this conclusion. Measuring the gluons contribution is the goal of the next generation of experiments in this field [9,10].

Parity violation in polarized electron proton scattering was proposed [12,13] as a way to measure the weak form factors, from which the vector matrix element $< N|\bar{s}\gamma_\mu s|N >$ can be deduced with the only assumption that isospin symmetry holds.

1.3 Form factors

The structure of a proton can be probed using the electromagnetic interaction. In that case the most general form of the matrix element which conserves current, parity and is invariant under time-reversal takes the following form :

$$< P|J_\mu^{EM}|P >= \bar{U}(F_1\gamma_\mu + \frac{i\sigma_{\mu\nu}q^\nu}{2M_N}F_2)U \tag{1}$$

where F_1 and F_2 are the Dirac and Pauli form factors and are functions of Q^2 and U and $\bar{U}$ are the nucleon spinors. In the literature, the Sachs form factors which are linear combinations of F_1 and F_2 are often encountered and will be used in the following :

$$G_E = F_1 - \frac{Q^2}{4M_n^2}F_2 \qquad G_M = F_1 + F_2 \tag{2}$$

If we now consider the weak interaction then parity is not conserved and the expression of matrix element has an additional axial-vector term :

$$< P|J_\mu^Z|P >= \bar{U}(F_1^Z\gamma_\mu + \frac{i\sigma_{\mu\nu}q^\nu}{2M_N}F_2^Z + G_A^Z\gamma_\mu\gamma_5)U \tag{3}$$

When probing the structure of a nucleon, the form factors can be expressed as the sum over the three lightest flavors [13,14]. For the electromagnetic form factors of a proton we have :

$$G^p_{E,M} = \frac{2}{3}G^u_{E,M} + \frac{1}{3}G^d_{E,M} + \frac{1}{3}G^s_{E,M} \tag{4}$$

Assuming isospin symmetry gives the following relation :

$$G^{u,(p)}_{E,M} = G^{d,(n)}_{E,M} \equiv G^u_{E,M} \qquad\qquad G^{s,(p)}_{E,M} = G^{s,(n)}_{E,M} \equiv G^s_{E,M} \tag{5}$$

And thus, the form factors for the neutron are :

$$G^n_{E,M} = \frac{1}{3}G^u_{E,M} + \frac{2}{3}G^d_{E,M} + \frac{1}{3}G^s_{E,M} \tag{6}$$

So, there are six quark-flavor form factors and four measurements available. Nevertheless, for the vector part of the neutral weak current the proton is probed with the same type of interaction but the coupling constants to the individual flavors are different :

$$\begin{aligned} G^{Z,p}_{E,M} = \; & (\frac{1}{4} - \frac{2}{3}\sin^2\theta_W)G^u_{E,M} + (-\frac{1}{4} + \frac{1}{3}\sin^2\theta_W)G^d_{E,M} \\ & +(-\frac{1}{4} + \frac{1}{3}\sin^2\theta_W)G^s_{E,M} \end{aligned} \tag{7}$$

Then, a measurement of the neutral weak form factors brings a supplementary constraint on the strange form factors. These form factors can be measured through parity violation in polarized electron scattering.

1.4 Parity violating asymmetry

The diagrams contributing to elastic electron proton scattering at tree level are the exchange of a virtual photon and the exchange of a Z^0 (see fig 1). The graph involving the weak interaction does not conserve parity and produces an asymmetry in the cross section for left and right electrons. As the Q^2 of the experiment is away from the Z pole the only sizeable contribution is through its interference with the one photon exchange :

$$\mathcal{A}_{PV} = \frac{\sigma^{\Leftarrow} - \sigma^{\Rightarrow}}{\sigma^{\Leftarrow} + \sigma^{\Rightarrow}} \simeq \frac{\mathcal{M}_\gamma\mathcal{M}_Z^*}{\mathcal{M}_\gamma^2} \tag{8}$$

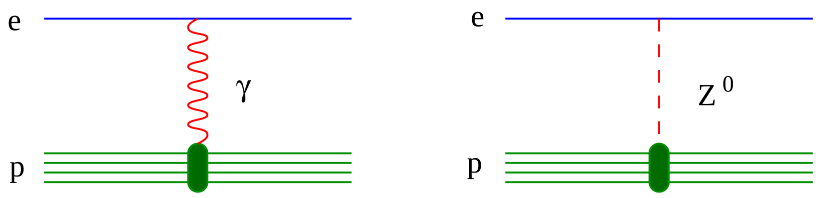

Figure 1: Graphs contributing at tree level to elastic electron proton scattering.

The asymmetry can be expressed as a function of the electromagnetic and weak form factors [5]:

$$\mathcal{A}_{PV} = \frac{-G_F Q^2}{\pi\alpha\sqrt{2}} \times \frac{\epsilon G_E^p G_E^Z + \tau G_M^p G_M^Z - \frac{1}{2}(1-4\sin^2\theta_W)\epsilon' G_M^p G_A^Z}{\epsilon (G_E^p)^2 + \tau (G_M^p)^2} \tag{9}$$

where ϵ, ϵ' and τ are kinematical parameters defined by

$$\tau = -\frac{Q^2}{4M_N^2} \quad \epsilon = [1 + 2(1+\tau)\tan^2\frac{\theta}{2}]^{-1} \quad \epsilon' = \sqrt{(1-\epsilon^2)(1+\tau)\tau} \tag{10}$$

The experiment took data at $Q^2 = 0.48$ (GeV/c)^2 and a scattering angle of $\theta = 12.5°$. At these kinematical point the term involving G_A^Z is of the order of (2.4±1.2) % and is treated as a systematic effect.

2 The HAPPEX experiment

The HAPPEX experiment measures the asymmetry of the cross section of elastic scattering of left and right polarized electrons off of a proton target. A schematic overview of the experiment is given on figure 2.

2.1 Polarized electron source

We have used an optically pumped bulk GaAs crystal as a polarized electron source. In this device, a 780 nm Laser is used to shine circularly polarized light onto the crystal. The laser is pulsed to the accelerator frequency (500 MHz) and the bunch-length is 50 picosecond. Left and right circular polarization of the light are obtained with a Pockels Cell by applying the voltage corresponding to the quarter wave retardation. For this experiment, about 80 Coulombs were drawn out of a single photocathode crystal with a stable polarization of 38 %.

The helicity is flipped at a 30 Hz frequency and is phase locked to the 60 Hz AC cycle. Helicity pulses are associated in pairs of which the second

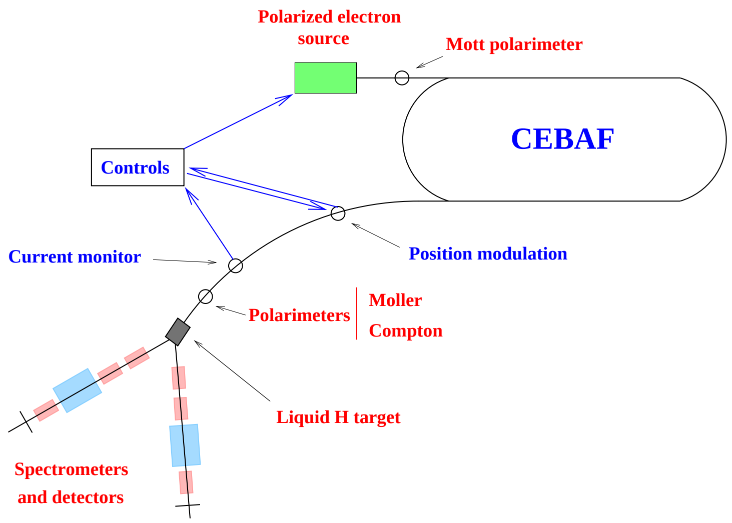

Figure 2: Overview of the HAPPEX experiment in the Hall A of Jefferson Lab

pulse has an opposite helicity as the first one. The helicity of the first one is chosen by a 24-bit pseudo-random number generator. The helicity signal is transfered delayed by 8 pairs and true helicity is determined afterwards in software. Asymmetries and differences are then calculated for pairs.

A half-wave plate can be inserted in the laser beam. As it swaps left and right helicities it reverses the sign of the experimental asymmetry and provides a useful systematic check. The half wave plate was put in or taken out after every 24 hours of full data taking.

2.2 Polarimeters

The polarization of the beam was measured using both a Mott and a Moller polarimeter. Both devices are intrusive and were run once a day. For the upcoming physics program it is also planned to use a Compton polarimeter [16].

The Mott polarimeter [15] is located at the 5 MeV stage of the accelerator. Mott scattering takes place in a thin gold foil and the largest analyzing power (~ 0.6) is at backward angle. Backscattered electrons are detected in four detectors associated in pairs. Each pair measures a component of the transverse polarization. The module of the polarization vector is determined by varying the orientation of the polarization vector using a Wien filter. The analyzing power varies with foil thickness because of rescatterring in the foil and leads to a 5 % systematic effect which is determined from the dispersion of the different extrapolation techniques. Other effects such as time and beam intensity dependence were studied and account for 3 % each. The total systematic error on the beam polarization is 7 %. Improvements are underway and a precision of 2 to 3 % should be achieved in the future.

The polarization of the beam was also measured using polarized Moller scattering. In this device, the polarization is determined from the asymmetry of the counting rates when the helicity of the beam is reversed. At the time the data presented here were taken the Moller polarimeter was being commissioned and the target magnetization was taken from the literature resulting in a 5 % systematic effect. Other systematic effects include backlash in the target rotation motor and intensity dependence. The total precision from the Moller measurement is also of the order of 7 % and a 3 % error is the goal for the future.

The value of the beam polarization was chosen as the average of the two measured values (which are in agreement) and the error was conservatively taken to be 7 %.

2.3 The spectrometers

After being accelerated to 3.355 GeV, the polarized electrons are extracted and deflected to the proton target. The target is a 15 cm long cell of liquid hydrogen cooled at 19 K. The cryogenic installation is able to evacuate the 500 Watts deposited in the target by a 100 μA electron beam. Tests performed prior to the experiment have shown that no significant boiling was induced in the target by the beam.

The two High Resolution Spectrometers (HRS) in Jefferson Lab's Hall A are used to detect the elastically scattered electrons. One property of the HRS is to separate spatially elastic form inelastic scattering. Thus, elastic scattering can be identified without reconstruction of the trajectories an enables integration of the signals.

The spectrometers were placed at the most forward scattering angle ($\theta = 12.5°$) and the field in the magnets (the configuration is QQDQ) was set to detect electrons at a quadri-momentum transfer $Q^2 = 0.48(\mathrm{GeV/c})^2$. These settings were chosen to maximize the figure of merit $(A(d\sigma)^{\frac{1}{2}})$ in a kinematical region where some models on strangeness predicted a sizeable effect [17,5].

To detect the scattered electrons total absorption electron calorimeters were placed in the focal plane of both spectrometers. These detectors are made of 5 layers of lead and leucite interleaved. The cerenkov light produced by the electron shower is detected by a 5 inch photomultiplier tube. The resolution of such a device is 14 % at the energy of the scattered electrons. Rates of 2 MHz were obtained and since the output current of the PMTs is integrated over the helicity pulse, the effect of the resolution is only to increase the time needed to achieve a given accuracy by less than a percent.

Data was also taken using the standard detector package of the HRSs in order to determine the averaged Q^2. Even if the spectrometers have a 10^{-4} momentum resolution, for the purpose of our experiment we only need precision of the order of a percent. An eventual contamination of background was also studied using the standard HRSs.

3 Beam instrumentation

One of the difficulties in measuring asymmetries at the level of 5 ppm is to control helicity correlated differences in any of the beam parameters such as intensity, position and energy. A great effort was put in developing experimental techniques to either annihilate the differences (as for beam intensity) or to measure how to correct for other them (as for position and energy).

3.1 Intensity feed-back

The beam intensity is measured using two microwave cavity monitors. Even if the counting rates are properly normalized using the beam current non-linearities in the detectors response might lead to a false asymmetry. This false asymmetry is found to be :

$$\mathcal{A}_{\mathrm{nl}} = \beta \cdot \mathcal{A}_{\mathrm{I}} \tag{11}$$

where β is the size of the non-linearities and $\mathcal{A}_{\mathrm{I}}$ is the asymmetry in beam intensity. Non-linearities can originate from numerous equipment such as current monitors and PMTs and ADCs and are not easy to estimate a priori. But if the asymmetry in beam current can be kept small enough then their influence would be negligible. To do so we have implemented a feed-back on the polarized source. A variation of the voltage applied to the Pockels cell creates a difference in laser power hitting the photocathode because of asymmetric transport of the laser light in the source optics. The effect is magnified by inserting a glass slide after the Pockels cell.

$$\mathcal{A}_{\mathrm{I}} = \mathcal{A}_{I_0} + \alpha \Delta V_{PC} \tag{12}$$

By changing the voltage on the Pockels cell one can annihilate the asymmetry in beam intensity (a few volts variation out of 2600 V is necessary). As some other effects can make $\mathcal{A}_{\mathrm{I}}$ vary, the procedure is repeated every five minutes. The slope α is measured once a day and variations of the order of 30 % were observed but did not prevent the feed-back from being efficient.

The averaged asymmetry in beam current observed is $0.5\ 10^{-6}$. An upper bound on the size of the non-linearities have been evaluated directly from the data $\beta < 4.\,10^{-3}$ and the systematic effect is then $2.\,10^{-9}$. In fact a bigger effect, $2.\,10^{-8}$, comes from the discrepancy between the measurements of the asymmetry in beam current performed by the two cavity monitors.

3.2 Position modulation

As differences in beam intensities are observed one can expect helicity correlated differences in beam position and energy as well. To calculate the asymmetry it is mandatory to evaluate the counting rate at the same point in beam phase space. It is therefore needed to know the sensitivity of counting rates with respect to variation in any of the beam parameters (the position in two points and the energy are sufficient). One beam position monitor located in a dispersive region of the machine is used to measure the energy. Two other monitors located 1.5 and 7 meters away from the target are used to measure the positions.

The sensitivity is measured by artificially modulating the beam parameters using magnetic coils C_j (one at a time) and recording the associated variation in beam parameters $\partial X_i/\partial C_j$ and in the rate seen by the detectors $\partial N_k/\partial C_j$. The correction to the counting rates is then :

$$\Delta N_k = \sum_i \sum_j \frac{\partial N_k}{\partial C_j} \left(\frac{\partial X_i}{\partial C_j}\right)^{-1} \Delta X_i \tag{13}$$

The helicity correlated differences observed, ΔX_i, are of the order of a few nanometers for the position coordinates and of $4.\,10^{-9}$ for the energy. Correlation coefficient are measured during one third of the data taking time. Very little variation on the sensitivity of the detectors was found over a month of data taking. The overall effect is found to be less than $2.\,10^{-8}$ and the correction was not applied.

4 Preliminary results

The integrated output of the PMTs are divided by the beam current and the asymmetry is calculated for each helicity pulse pairs. The averaging is performed by weighting each pair by the corresponding beam current. In these conditions the experimental asymmetry is found to be :

$$\mathcal{A}_{\rm exp}({\rm ppm}) = -5.64 \pm (0.75)_{\rm stat} \tag{14}$$

No corrections due to false asymmetries were needed. The only cuts applied in the analysis are meant to ensure that the beam was on and that the spectrometers and the target were functioning. The total fraction of helicity pairs cut is 20 %. To determine the parity violating asymmetry, the polarization of the beam is taken to be $P_e = 0.388 \pm 0.027$ and thus

$$\mathcal{A}_{\rm PV}({\rm ppm}) = \frac{\mathcal{A}_{\rm exp}}{P_e} = -14.5 \pm (2.0)_{\rm stat} \pm (1.1)_{\rm syst} \tag{15}$$

The biggest source of error is the polarization of the beam. Other sources of error are listed in table 1. To determine the asymmetry expected from the standard model we have used the dipole approximation for the electromagnetic form factors :

$$G_E^p = \frac{1}{(1+\frac{Q^2}{m_D^2})^2} \qquad G_M^p = \mu_p G_E^p \qquad G_M^n = \mu_n G_E^p \tag{16}$$

where $m_D = 0.842$ GeV, $\mu_p = 2.79$ and $\mu_n = -1.91$. For the neutron electric form factor we used the Galster parameterization [18] :

$$G_E^n = \frac{-\mu_n \tau G_E^p}{1+\lambda_g \tau} \tag{17}$$

where $\lambda_g = 5.6$. With this parameterization we obtain :

$$\mathcal{A}_{\rm SM}({\rm ppm}) = -15.8 \pm (1.7)_{\rm th} \tag{18}$$

where the error is determined by varying the form factors by their measured errors (50 % for G_E^n and 5 % for the others, see table 1). The poor knowledge that we have on the neutron electric form factor, G_E^n, is the dominant contribution to the error on the expected asymmetry. Experiments are planned or underway at Jefferson Lab to measure G_E^n at the 20 % level.

On figure 3 we have represented the asymmetries obtained for the two detectors and for the two states of half-wave plate settings and their average value. The result is compatible with the standard model prediction. From the observed difference we have determined a combination of the strange form factors. Using the parameterization of the electromagnetic form factors mentioned above we obtain :

$$G_E^S + \frac{\tau \mu_P}{\epsilon} G_M^s \simeq \frac{\mathcal{A}_{\rm PV} - \mathcal{A}_{\rm SM}}{-G_F Q^2/\pi\alpha\sqrt{2}} \epsilon G_E^p \left(1 + \frac{\tau \mu_P^2}{\epsilon}\right) \tag{19}$$

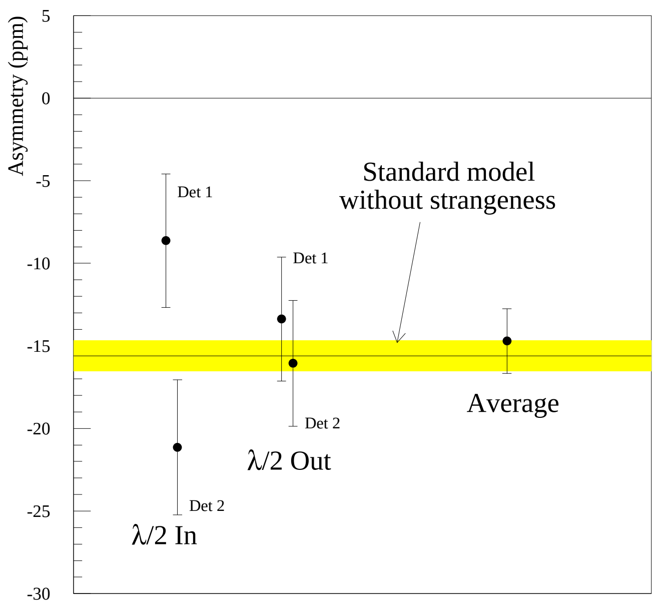

Figure 3: Measured asymmetries for the two detectors and for the two half-wave plate settings (corrected for the sign) and their average value. The shaded band represents the value expected from the standard model and the measurement of the electromagnetic form factors.

That is :

$$G_E^s + 0.39\, G_M^s = 0.023 \pm 0.049 \qquad (Q^2 = 0.48\, GeV^2/c^2) \tag{20}$$

This value is consistent with small effects from strange quarks and is only two standard deviations away from models predicting a larger contribution from strange quarks [17,19].

5 Conclusions

We have presented here the preliminary results of a measurement of the strange form factors of the nucleon. The result we found is compatible with a small effect of strange quarks. It is in agreement with the result from the Sample experiment [20] which ran at a lower Q^2 and with previous neutrino scattering experiments [11]. A better precision will allow to discriminate some of the

Errors in the determination of $\mathcal{A}_{\rm PV}$	(ppm)
beam polarization	1.03
background	0.29
helicity correlations	0.03
total	1.07
Errors in the determination of $\mathcal{A}_{\rm SM}$	(ppm)
G_E^n	1.49
other form factors	0.72
determination of Q^2	0.44
radiative corrections	0.30
total	1.73
Total	**2.03**

Table 1: Summary of experimental and theoretical errors entering the measurement.

models and help find the right degrees of freedom for an effective theory. The experiment will run again in 1999 and we expect an improvement in the precision by a factor of 2. There is a wide physics program ahead using parity violation in electron scattering especially at Jefferson Lab [22,21] where the beam is of unprecedented quality and also in other labs [20,23].

References

1. D. Kaplan and A. Manohar, *Nucl. Phys.* B **310**, 527 (1988).
2. EMC collaboration, J. Ashman et al., Phys. Lett. **206**, 364 (1988).
3. BCDMS collaboration, H. Abramowicz et al., Z. Physik **C15**, 19 (1982).
4. CCFR collaboration, A. O. Bazarko et al., Z. Physik **C65**, 189 (1995).
5. M. Musolf et al., Phys. Rep. **239** 1 (1994) and references therein.
6. SMC collaboration, D. Adams et al., Phys. Rev **D56**, 5330 (1997) and references therein.
7. E154 collaboration, K. Abe et al., Phys. Rev. Lett. **79**,26 (1997) and references therein.
8. HERMES collaboration, A. Airapetian et al., hep-ex/9807015 and references therein.
9. COMPASS collaboration, G. Baum et al., CERN-SPSLC-96-14.
10. PHENIX/Spin collaboration, BNL-PROPOSAL-R5 and STAR collaboration, BNL-PUB-5347.
11. G. T. Garvey et al., Phys. Rev. **C28**, 761 (1993).
12. R. D. McKeown, *Phys. Lett.* B **219**, 140 (1989).

13. D. H. Beck, *Phys. Rev.* D **39**, 3248 (1989).
14. R. D. McKeown, *Nucl. Phys.* A **631**, 42c-55c (1998).
15. J. Price, these proceedings.
16. T. Pussieux, these proceedings.
17. R. L. Jaffe, Phys. Lett. **B229** 275 (1989).
18. S. Galster et al., Nucl. Phys **B32**, 221 (1971).
19. N. W. Park et al., Phys. Rev. **D43**, 869 (1991).
20. SAMPLE collaboration, B. Mueller et al., Phys. Rev. Lett. **78**, 3824 (1997).
21. Jefferson Lab experiment E91-004, E. J. Beise, spokesperson.
22. Jefferson Lab experiment E91-017, D. Beck, spokesperson.
23. Mainz experiment A4, D. von Harrach, spokesperson.